

Charm spectroscopy in the *BABAR* experiment

LOREDANA LOPEZ⁽¹⁾(²)

⁽¹⁾ *Dipartimento di Fisica, University of Study of Bari, Via Amendola173, I-70126 Bari,Italy*

⁽²⁾ *INFN, Sezione di Bari I-70126 Bari,Italy*

Summary. — New and recent results are presented on charm spectroscopy from *BABAR* experiment at SLAC. In particular, new estimates of the $D_{s0}^*(2317)^+$, $D_{s1}^*(2460)^+$ and $D_{s1}^*(2536)^+$ meson properties and the discovery of a new D_s^+ meson at 2.856 GeV/ c^2 decaying to DK, are addressed. These analysis have been performed using $e^+e^- \rightarrow c\bar{c}$ continuum events on a data sample corresponding to an integrated luminosity of about 240 fb⁻¹.

PACS 14.40.Lb – Charmed mesons.

PACS 13.25.Ft – Decays of charmed mesons.

PACS 12.40.Yx – Hadron mass models and calculations.

1. – Introduction

In the last few years we observed a new interest in the charm spectroscopy with more than a dozen new states being reported and hundreds of new theoretical investigations being published. The advance of the B-factory [1][2] with their rich charm data sample, has proven crucial to the discovery and investigation of new charm hadron states, but other experiments have confirmed and complemented the B-factory observations.

The *BABAR* experiment, at the PEP-II B-factory, is designed to perform precision measurements of CP violation in the B meson decays. Moreover a much broader physics reach is available and an extensive program of meson spectroscopy has been performed. In the following we will present some recent *BABAR* results about the spectroscopy of these new states.

2. – New Measurements of D_{sJ} properties

The D_s^+ mass spectrum was reasonably well described by potential models [3] up to recent years, but the recently discovered $D_{s0}^*(2317)^+$ and $D_{s1}^*(2460)^+$ mesons do not confirm conventional models of $c\bar{s}$ meson spectroscopy. The possibility that these are exotic states [4], [5] has attracted considerable experimental and theoretical interest and has focused renewed attention on the subject of charmed-meson spectroscopy in general.

An updated analysis of these two states using 232 fb^{-1} of $e^+e^- \rightarrow c\bar{c}$ has been performed [6]. The following final states have been considered: $D_s^+\pi^0$, $D_s^+\gamma$, $D_s^{*+}\pi^0$, $D_{s0}^*(2317)^+\gamma$, $D_s^+\pi^0\pi^0$, $D_s^+\gamma\gamma$, $D_s^{*+}\gamma$ and $D_s^+\pi^+\pi^-$. Charged conjugated states are implicitly included here and throughout. Moreover, the $D_s^+\pi^+$ and $D_s^+\pi^-$ systems have been examined in search for partner states of the $D_{s0}^*(2317)^+$ predicted by some four-quark models.

The $D_{s0}^*(2317)^+$ is only observed in its decay to $D_s^+\pi^0$. Shown in fig. 1(left) is the invariant mass distribution of the $D_s^+\pi^0$ combinations. Beside clear $D_s^*(2112)^+$ and $D_{s0}^*(2317)^+$ signals, a broad structure peaking at $2.17 \text{ GeV}/c^2$ is apparent. This structure is identified to be a reflection arising from $D_s^{*+} \rightarrow D_s^+\gamma$ decays. Another reflection is associated with $D_{s1}(2460)^+ \rightarrow D_s^{*+}\pi^0$ decays and is underlying the $D_{s0}^*(2317)^+$ signal. An unbinned likelihood fit accounting for signals, reflections, combinatorial background and a hypothetical $D_{s1}(2460)^+$ contribution, is applied to this mass distribution in order to extract the parameters and yield of the $D_{s0}^*(2317)^+$ signal and upper limits on $D_{s1}(2460)^+$ decay. The shapes of the signals and reflections have been derived from Monte Carlo (MC) simulations. The resulting $D_{s0}^*(2317)^+$ mass is shown in table I. Moreover, a search has been performed in order to find neutral ($D_s^+\pi^-$) and double charged ($D_s^+\pi^+$) partners for $D_{s0}^*(2317)^+$: no indication has been found for such a states as is shown in fig 1(right).

On the other hand, the $D_{s1}(2460)^+$ is observed in its decays to $D_s^+\gamma$, $D_s^+\pi^0\gamma$ and $D_s^+\pi^+\pi^-$.

The $D_s^+\gamma$ mass distribution is shown in fig. 2. Clear evidence for $D_{s1}(2460)^+$ can be seen together with the reflection of $D_{s0}^*(2317)^+ \rightarrow D_s^+\pi^0$ with a missing γ .

For the decay to $D_s^+\pi^0\gamma$, the two subresonant $D_s^{*+}\pi^0$ and $D_{s0}^*(2317)^+\gamma$ decay modes,

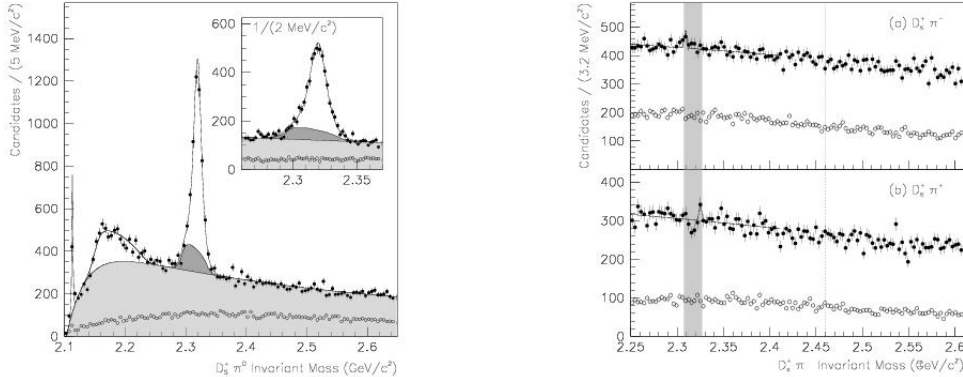


Fig. 1. – Left. The invariant mass distribution for (solid points) $D_s^+\pi^0$ candidates and (open points) the equivalent using the D_s^+ sidebands. Included in this fit is (light shade) a contribution from combinatorial background and (dark shade) the reflection from $D_{s1}(2460)^+ \rightarrow D_s^*(2112)^+\pi^0$ decay. Right. The invariant mass distribution (solid points) of (a) $D_s^+\pi^-$ (b) $D_s^+\pi^+$ candidates and (open points) the equivalent for the D_s^+ sidebands. The shaded regions indicate the range of assumed $D_{s0}^*(2317)^{++}$ and $D_{s0}^*(2317)^0$ masses

overlapping in their kinematics and thus difficult to disentangle, have been considered. The decay to $D_s^+ \pi^0 \gamma$ is found to proceed entirely through $D_s^{*+} \pi^0$. However, the two modes are included together in the analysis, which makes the measured ratios of branching fractions directly comparable to previous measurements, where a possible contribution of $D_{s0}^*(2317)^+ \gamma$ has not been taken into account. The $D_s^+ \pi^0 \gamma$ mass distribution in the $D_s^*(2112)^+$ signal region and sidebands are shown in fig. 3(left). A clear $D_{s1}(2460)^+$ signal can be seen, together with reflections from $D_{s0}^*(2317)^+$ (underlying the $D_{s1}(2460)^+$ signal) and $D_s^*(2112)^+$.

The $D_s^+ \pi^+ \pi^-$ final state includes only charged particles. Since the performance of the tracking system is well understood, a precise measurement of the $D_{s1}(2460)^+$ mass is provided from this decay mode. The invariant mass distribution of the $D_s^+ \pi^+ \pi^-$ candidates is shown in fig. 3(right) where clear peaks from $D_{s1}(2460)^+$ and $D_{s1}(2536)^+$ decay are apparent. The signal yields and mean values have been determined from an unbinned ML fit accounting for the two signals, a hypothetical $D_{s0}^*(2317)^+$ contribution and com-

TABLE I. – A summary of the combined mass and width results. The first quoted uncertainty is statistical and the second is systematic.

Particle	Mass (MeV/ c^2)	Γ (MeV)
$D_{s0}^*(2317)^+$	$2319.6 \pm 0.2 \pm 1.4$	< 3.8
$D_{s1}(2460)^+$	$2460.1 \pm 0.2 \pm 0.8$	< 3.5
$D_{s1}(2536)^+$	$2534.6 \pm 0.3 \pm 0.7$	< 2.5

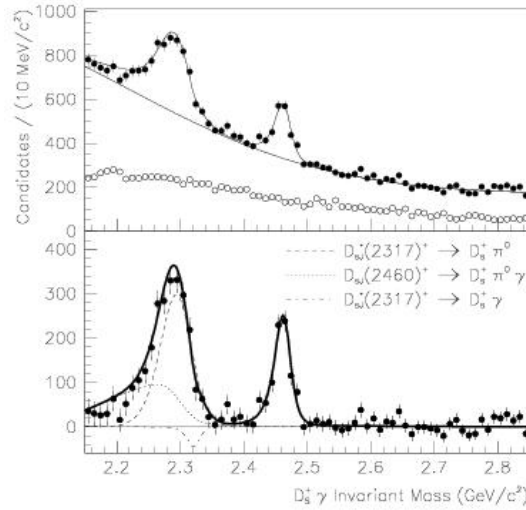


Fig. 2. – The $D_s^+ \gamma$ invariant mass distribution. The solid points in the top plot are the mass distribution. The open points are the D_s^+ sidebands, scaled appropriately. The bottom plot shows the same data after subtracting the background curve from the fit. Various contributions to the likelihood fit are also shown.

binatorial background. The signal line shapes have been derived from MC simulation. In addition, it has been possible to estimate the mass and limits on the intrinsic width of the $D_{s1}(2536)^+$ from such an analysis.

The mass and width results for the $D_{s0}^*(2317)^+$, $D_{s1}(2460)^+$, and $D_{s1}(2536)^+$ mesons are summarized in table I. The $D_{s1}(2460)^+$ mass is the average of that obtained from the $D_s^+\gamma$, $D_s^+\pi^0\gamma$, and $D_s^+\pi^+\pi^-$ final states, although the latter measurement dominates in the average due to superior systematic uncertainties.

A summary of the branching-ratio and limits is displayed in table II.

3. – Measurement of D_s^+ and $D_{s1}(2460)^+$ Branching Fractions.

This analysis uses $\Upsilon(4S) \rightarrow B\bar{B}$ events in which either a B^+ or a B^0 meson decays into a fully reconstructed hadronic final state [7]. The recoiling B meson, on the other hand, decays to two charm mesons, *i.e.* $\bar{B} \rightarrow D_{\text{meas}}D_X$. Here D_{meas} represents a fully reconstructed $D^{(*)+,0}$ or $D_s^{(*)-}$ meson, and the mass and momentum of the D_X are inferred from the kinematics of the two-body B decay. This study allows measurements of B branching fractions without any assumption on the decays of the D_X . The measurements are based on an integrated luminosity of 210.5 fb^{-1} . From two separate classes of events with $D_{\text{meas}} = D_s^{(*)-}$ and with $D_X = D_s^{(*)-}$ we measure the branching fraction of $D_s^- \rightarrow \phi\pi^-$, which has important implications for a wide range of D_s and B physics. Furthermore, we select final states with $D_X = D_{s1}(2460)^-$ and combine with the BABAR measurements of $\mathcal{B}(\bar{B} \rightarrow D^{(*)+,0}D_{s1}(2460)^-) \times \mathcal{B}(D_{s1}(2460)^- \rightarrow D_s^{*-}\pi^0)$ and $\mathcal{B}(B \rightarrow D^{(*)+,0}D_{s1}(2460)^-) \times \mathcal{B}(D_{s1}(2460)^- \rightarrow D_s^-\gamma)$ [8], thus extracting for the first time the absolute branching fractions of this recently observed state.

One example of distribution of m_ν is shown in fig. 4. We obtain the following branch-

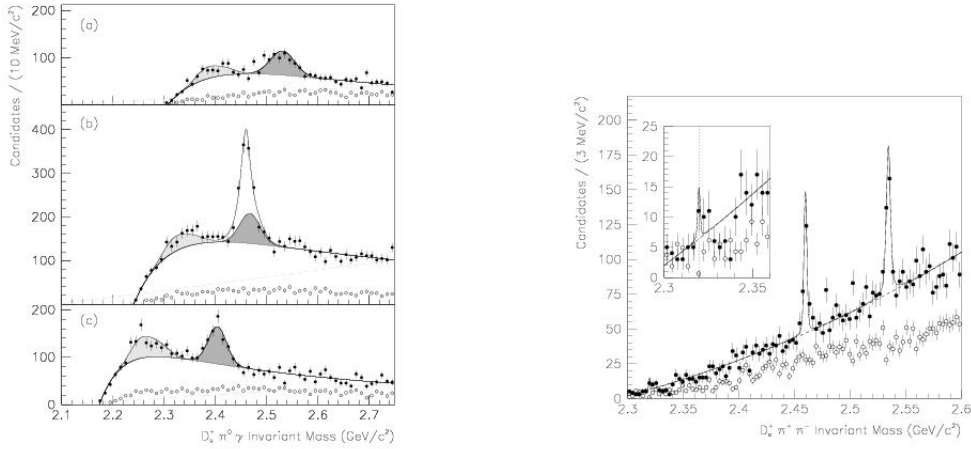


Fig. 3. – Left. The invariant mass distribution of $D_s^+\pi^0\gamma$ candidates in the (a) upper, (b) signal, and (c) lower in the $D_s^+\gamma$ mass selection windows close to $D_s^*(2112)^+$ for (solid points) the D_s^+ signal and (open points) D_s^+ sideband samples. The dark gray (light gray) region corresponds to the predicted contribution from the $D_{s0}^*(2317)^+$ ($D_s^*(2112)^+$) reflection. Right. The invariant mass distribution of (solid points) $D_s^+\pi^+\pi^-$ candidates and (open points) the equivalent using the D_s^+ sidebands. The dotted line in the insert indicates the $D_{s0}^*(2317)^+$ mass.

TABLE II. – A summary of branching-ratio results. The first quoted uncertainty for the central value is statistical and the second is systematic. The limits correspond to 95% CL.

Decay Mode	Central Value			Limit
$\mathcal{B}(D_{s0}^*(2317)^+ \rightarrow X)/\mathcal{B}(D_{s0}^*(2317)^+ \rightarrow D_s^+ \pi^0)$				
$D_s^+ \gamma$	$-0.02 \pm$	$0.02 \pm$	0.08	< 0.14
$D_s^+ \pi^0 \pi^0$	$0.08 \pm$	$0.06 \pm$	0.04	< 0.25
$D_s^+ \gamma \gamma$	$0.06 \pm$	$0.04 \pm$	0.02	< 0.18
$D_s^*(2112)^+ \gamma$	$0.00 \pm$	$0.03 \pm$	0.07	< 0.16
$D_s^+ \pi^+ \pi^-$	$0.0023 \pm$	$0.0013 \pm$	0.0002	< 0.0050
$\mathcal{B}(D_{s1}(2460)^+ \rightarrow X)/\mathcal{B}(D_{s1}(2460)^+ \rightarrow D_s^+ \pi^0 \gamma)$ [a]				
$D_s^+ \pi^0$	$-0.023 \pm$	$0.032 \pm$	0.005	< 0.042
$D_s^+ \gamma$	$0.337 \pm$	$0.036 \pm$	0.038	—
$D_s^*(2112)^+ \pi^0$	$0.97 \pm$	$0.09 \pm$	0.05	> 0.75
$D_{s0}^*(2317)^+ \gamma$	$0.03 \pm$	$0.09 \pm$	0.05	< 0.25
$D_s^+ \pi^0 \pi^0$	$0.13 \pm$	$0.13 \pm$	0.06	< 0.68
$D_s^+ \gamma \gamma$	$0.08 \pm$	$0.10 \pm$	0.04	< 0.33
$D_s^*(2112)^+ \gamma$	$-0.02 \pm$	$0.08 \pm$	0.10	< 0.24
$D_s^+ \pi^+ \pi^-$	$0.077 \pm$	$0.013 \pm$	0.008	—
$\sigma(D_{s0}^*(2317)^{++})/\sigma(D_{s0}^*(2317)^+) \times$				
$\mathcal{B}(D_{s0}^*(2317)^{++} \rightarrow X)/\mathcal{B}(D_{s0}^*(2317)^+ \rightarrow D_s^+ \pi^0)$	—			< 0.017
$\sigma(D_{s0}^*(2317)^0)/\sigma(D_{s0}^*(2317)^+) \times$				
$\mathcal{B}(D_{s0}^*(2317)^0 \rightarrow X)/\mathcal{B}(D_{s0}^*(2317)^+ \rightarrow D_s^+ \pi^0)$	—			< 0.013

[a] Denominator includes both $D_s^*(2112)^+ \pi^0$ and $D_{s0}^*(2317)^+ \gamma$ channels.

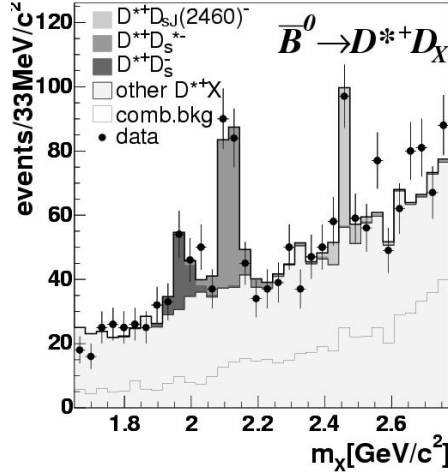


Fig. 4. – One example of distribution of m_X for $\bar{B}^0 \rightarrow D^{*+} D_X$. Fitted $\bar{B}^0 \rightarrow D^{(*)+},^0 D_s^{(*)-}$ and $\bar{B} \rightarrow D^{(*)+},^0 D_{s1}(2460)^-$ signal contributions and background components, are overlaid to the data points.

ing fractions:

$$\begin{aligned}\mathcal{B}(D_{s1}(2460)^- \rightarrow D_s^{*-} \pi^0) &= (56 \pm 13_{\text{stat.}} \pm 9_{\text{syst.}})\%, \\ \mathcal{B}(D_{s1}(2460)^- \rightarrow D_s^- \gamma) &= (16 \pm 4_{\text{stat.}} \pm 3_{\text{syst.}})\%, \\ \mathcal{B}(D_s^- \rightarrow \phi \pi^-) &= (4.62 \pm 0.36_{\text{stat.}} \pm 0.50_{\text{syst.}})\%.\end{aligned}$$

Our results show that the $D_{s1}(2460)^-$ meson decays via photon or π^0 emission to $D_s^{(*)-}$ in $(72 \pm 19)\%$ of the cases.

4. – Observation of a new D_{sJ} meson at a mass of 2.860 GeV/ c^2 .

We report here on a new $c\bar{s}$ state observed in the decay channels $D^0 K^+$ and $D^+ K_S^0$ [9]. This analysis is based on a 240 fb^{-1} data sample. We observe three inclusive processes:

- (1) $e^+e^- \rightarrow D^0 K^+ X, D^0 \rightarrow K^- \pi^+$
- (2) $e^+e^- \rightarrow D^0 K^+ X, D^0 \rightarrow K^- \pi^+ \pi^0$
- (3) $e^+e^- \rightarrow D^+ K_S^0 X, D^+ \rightarrow K^- \pi^+ \pi^+, K_S^0 \rightarrow \pi^+ \pi^-$

Selecting events in the D signal regions, fig. 5 shows the $D^0 K^+$ invariant mass distributions for channels (1) and (2), and the $D^+ K_S^0$ invariant mass distribution for channel (3).

The three mass spectra in fig. 5 present similar features:

- A single bin peak at 2.4 GeV/ c^2 , due to a reflection from the decays of $D_{s1}(2536)^+$ to $D^{*0} K^+$ or $D^{*+} K_S^0$ in which the π^0 or γ , from the D^* decay, is missed;

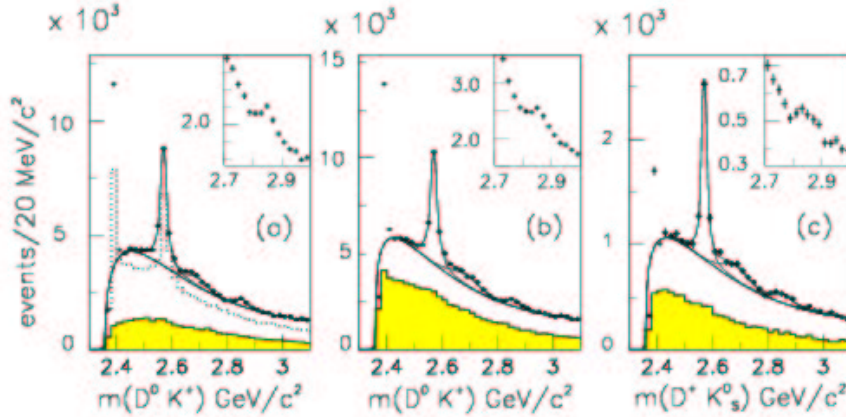


Fig. 5. – The DK invariant mass distributions for (a) $D_{K-\pi^+}^0 K^+$, (b) $D_{K-\pi^+\pi^0}^0 K^+$ and (c) $D_{K-\pi^+\pi^+}^+ K_S^0$. The shaded histograms are for the D -mass sideband regions. The dotted histogram in (a) is from $e^+e^- \rightarrow c\bar{c}$ Monte Carlo simulations with an arbitrary normalization. The insets show an expanded view of the 2.86 GeV/ c^2 region.

- A broad structure peaking at a mass of approximately $2.7 \text{ GeV}/c^2$;
- An enhancement around $2.86 \text{ GeV}/c^2$. This can be seen better in the expanded views shown in the insets of fig. 5.

No significant structures are present in the distribution obtained for D sideband regions. Table III summarizes the χ^2 probabilities, the number of $D_{sJ}(2860)^+$ events (with statistical and systematic errors) and the $D_{sJ}(2860)^+$ statistical significances from the three separate fits to the DK mass spectra.

Fig. 6 shows the background-subtracted $D_{K-\pi^+}^0 K^+$, $D_{K-\pi^+\pi^0}^0 K^+$, and $D_{K-\pi^+\pi^+}^+ K_s^0$ invariant mass distributions in the $2.86 \text{ GeV}/c^2$ mass region. fig. 6(d) shows the sum of the three mass spectra.

The possibility that the signal is produced by reflections from D^* decays or misidentification of kaons, pions and protons has been carefully investigated and excluded. Also possible reflections from other charmed particles decays can be ruled out as source of signal since it does not show up in the distributions from MC simulation of $e^+e^- \rightarrow c\bar{c}$ events which includes all known charmed particles and decays (see fig. 5(a)).

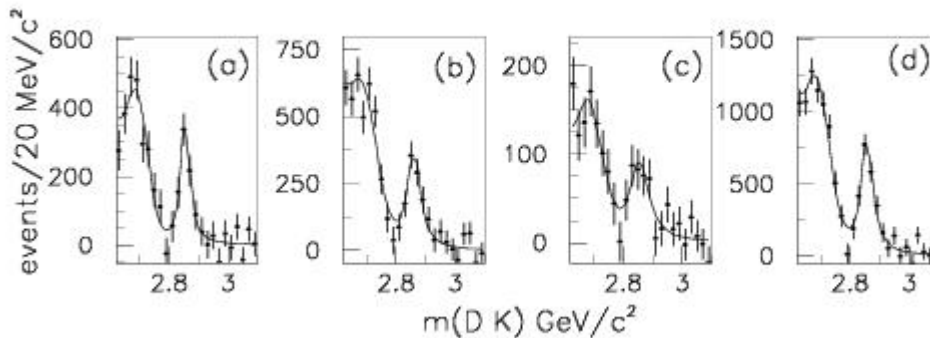


Fig. 6. – Background-subtracted DK invariant mass distributions for (a) $D_{K-\pi^+}^0 K^+$, (b) $D_{K-\pi^+\pi^0}^0 K^+$, (c) $D_{K-\pi^+\pi^+}^+ K_s^0$, and (d) the sum of all modes in the $2.86 \text{ GeV}/c^2$ mass region.

TABLE III. – χ^2 probabilities, $D_{sJ}(2860)^+$ event yields and statistical significances from the three separate fits to the DK mass spectra.

Channel	χ^2 probability (%)	$D_{sJ}(2860)^+$ events	Statistical significance
$D_{K-\pi^+}^0 K^+$	17	$886 \pm 134 \pm 49$	6.2σ
$D_{K-\pi^+\pi^0}^0 K^+$	3	$1146 \pm 157 \pm 78$	6.5σ
$D_{K-\pi^+\pi^+}^+ K_s^0$	21	$371 \pm 84 \pm 53$	3.7σ

We obtain the mass and width of $D_{s2}^*(2573)^+$:

$$m(D_{s2}^*(2573)^+) = (2572.2 \pm 0.3 \pm 1.0), \Gamma(D_{s2}^*(2573)^+) = (27.1 \pm 0.6 \pm 5.6) \text{ MeV}/c^2,$$

where the first errors are statistical and the second systematic.

For the new state we find:

$$m(D_{sJ}(2860)^+) = (2856.6 \pm 1.5 \pm 5.0), \Gamma(D_{sJ}(2860)^+) = (47 \pm 7 \pm 10) \text{ MeV}/c^2.$$

The decay of the $D_{sJ}(2860)^+$ meson to DK , implies that it has a natural-spin parity. It has been suggested this state could be a radial excitation [10] of the $D_{s0}^*(2317)^+$ meson, but other assignement cannot be excluded.

The broad structure around $2.7 \text{ GeV}/c^2$ has been parametrized with a Gaussian. In a fit which assumes the $X(2690)^+$ as an additional resonance, its parameters are:

$$m(X(2690)^+) = (2688 \pm 4 \pm 3), \Gamma(X(2690)^+) = (112 \pm 7 \pm 36) \text{ MeV}/c^2.$$

REFERENCES

- [1] B. AUBERT *et al.*: Nucl. Instr. Methods Phys. Res., Sect. A **479**,(2002) 1
- [2] A. ABASHIAN *et al.*: Nucl. Instr. Methods Phys. Res., Sect. A **479**,(2002) 117
- [3] S. GODFREY AND N. ISGUR: Phys. Rev.,**D32**,(1985)189
- [4] T. BARNES,F.E. CLOSE AND H.J. LIPKIN: Phys. Rev.**D68**,(2003) 054006
- [5] H.J. LIPKIN: Phys. Rev.**B580**,(2004) 50
- [6] B. AUBERT *et al.*: Phys. Rev.**D74**,(2006) 032007
- [7] B. AUBERT *et al.*: Phys. Rev. **D74**,(2006) 031103
- [8] B. AUBERT *et al.*: Phys. Rev. Lett., **93**,(2004) 181801
- [9] B. AUBERT *et al.*: Phys. Rev. Lett., **95**,(2006) 222001
- [10] E. VAN BEVEREN AND G.RUPP: Phys. Rev. Lett., **97**,(2006) 202001